

Active Displacement Feedback Control of a Smart Beam: Analytic and Numerical Solutions

C. SPIER¹, I.S. SADEK², J. C. BRUCH, JR.³, J. M. SLOSS⁴, S. ADALI⁵

Abstract: Active vibration control of a smart beam with integrated piezoceramic actuator and sensor patches is considered. An analytical solution of this problem is worked out for the case of the controlled beam including the mass and stiffness of the piezoceramic patches. The equation of motion for the controlled beam includes Heaviside functions and derivatives of the Heaviside function due to finite patch lengths. This makes the problem difficult to solve using conventional methods. An integral equation is introduced, where the eigensolutions of the integral equation are eigensolutions of the differential equation of motion for the controlled beam. A finite element model of a controlled beam is also formulated. The model contains modified beam element mass and stiffness matrices to account for the piezo patches and control effect. Two case studies are presented and the first three natural frequencies and mode shapes are found using the finite element and integral equation solutions. The results from the integral equation solution match very closely the results from the finite element solution.

Keywords: Displacement feedback control, piezoceramic actuators and sensors, smart structures

1. INTRODUCTION

In the present work, an analytical solution is proposed to find the natural frequencies and mode shapes for a controlled beam with piezoceramic sensor and actuator patches. Active vibration control is implemented using closed-loop displacement feedback with piezoceramic patches. Previous solutions neglect the mass and stiffness of the piezo patches, which can be significant if piezoceramic materials are used.

The specific controlled structure to be studied is a cantilever beam with a piezoceramic sensor bonded to the top surface of the beam and a piezoceramic actuator bonded to the bottom surface of the beam. The sensor on the top detects a strain when the beam is vibrating and the output voltage signal of the sensor is amplified and sent to the actuator. The signal sent to the actuator attempts to counteract the vibration of the beam and control its motion. Vibration control using piezoelectric patches is a widely researched topic. However, there is no analytical solution available for an actively controlled beam with

finite length patches where the patch stiffness and mass are included in the equation of motion. In [1], Tzou derives the governing equations used in the analysis of an actively controlled structure. The governing equations include the sensor voltage created due to a vibrating beam and the externally applied moment the piezo actuator creates on the beam. The sensor voltage and the applied moment are the basis for active control and show up in the equation of motion.

An equation of motion including the stiffness and mass of the piezo patches is derived by Banks *et al.* [2]. In [2], piezoceramic patches are used for the damage detection of a structure where the stiffness and mass have been changed due to damage. The motive behind Banks *et al.* [2] is different than what is desired for active vibration suppression, but the equation of motion for a cantilever beam with piezo patches is the same for both cases.

There have been several results (see e.g. [3]) for controlled beams using piezoceramic actuators. However, these results only use piezo patches as actuators and do not use them as sensors. A constant voltage is applied to the actuators in these cases and closed-loop control is imposed where the sensor is continuously sending a changing signal to the actuator. Tani *et al.* [4] performed an experiment using a gap sensor to detect the displacement of the beam and the information is converted to voltage and fed to piezoceramic actuators.

Analytical solutions have been obtained using an integral equation approach for an actively controlled beam [5-6]. Sloss *et al.* [5] derive an analytic solution to find the natural frequencies for finite length piezo patches, but does not include the mass and stiffness of the patch. The solution for using multiple piezo sensor and actuator patches, also not including the stiffness and mass of the patches, is found in [6].

2. PROBLEM FORMULATION

The cantilever beam is uniform with rectangular cross section and is clamped at $x=0$ and has a free end at $x=l$. Piezoceramic patches are bonded to the top and bottom surfaces of the beam as shown in Figure 1.

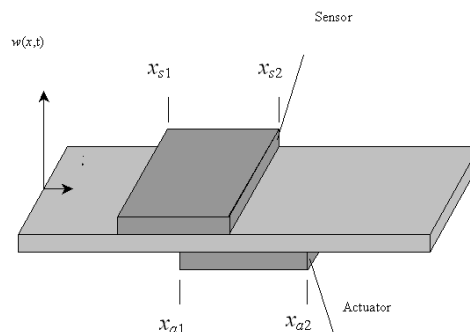


Fig. 1: Schematic of sensor and actuator patch locations

¹ Department of Mechanical Engineering, University of California, Santa Barbara, CA 93106, USA (spier@engineering.ucsb.edu)

² Department of Mathematics and Statistics, American University of Sharjah, United Arab Emirates (sadek@aus.edu)

³ Department of Mechanical Engineering and Department of Mathematics, University of California, Santa Barbara, CA 93106, USA (jcb@engineering.ucsb.edu)

⁴ Department of Mathematics, University of California, Santa Barbara, CA 93106 USA (JMSLOSS@SILCOM.COM)

⁵ School of Mechanical Engineering, University of KwaZulu-Natal, Durban, South Africa (adali@ukzn.ac.za)

The piezoceramic layers are considered to be perfectly bonded to the top and bottom surfaces of the elastic beam and the physical properties of the bonding material are not considered. Also, the effective axis of the piezoelectric layers is aligned with the x -axis to ensure the maximum piezoelectric effects in sensor and actuator applications. The location of the sensor is given by $x_{s1} \leq x \leq x_{s2}$ and the location of the actuator is given by $x_{a1} \leq x \leq x_{a2}$. The transverse deflection of the beam is represented by $w(x,t)$ and the equation of motion of the actively controlled beam with collocated sensor and actuator patches is

$$\rho(x) \frac{\partial^2 w}{\partial t^2} + L[w] = 0 \quad (2.1)$$

where the operator L is defined by

$$L[w] = \frac{\partial^2}{\partial x^2} \left(\alpha(x) \frac{\partial^2 w}{\partial x^2} \right) - b \xi \left(\frac{\partial w}{\partial x} \right)_{x_{s1}}^{x_{s2}} S''(x) \quad (2.2)$$

where the primes refer to differentiation with respect to x and $\alpha(x)$, $\rho(x)$, $S(x)$ and ξ are given by

$$\rho(x) = \rho_b A_b + 2\rho_p A_p [H(x-x_{a1}) - H(x-x_{a2})] \quad (2.3)$$

$$\alpha(x) = E_b I_b + 2E_p I_p [H(x-x_{a1}) - H(x-x_{a2})] \quad (2.4)$$

$$S(x) = H(x-x_{a1}) - H(x-x_{a2}) \quad (2.5)$$

$$\xi = - \frac{GE_a h_s r_a d_{31,a} h_{31,s}}{x_{s2} - x_{s1}} \quad (2.6)$$

for $0 < x < l$ and $t > 0$, where the subscripts b , a and s refer to the properties of the beam, the piezoceramic actuator material and the piezoceramic sensor material, respectively, and ρ is the density, A is the cross section area, E is the elastic modulus, I is the moment of inertia, b is the beam width, and $H(x)$ is the Heaviside function. In equations (2.3)-(2.4), the patch properties are now given by $E_p = E_a = E_s$, $I_p = I_a = I_s$, $\rho_p = \rho_a = \rho_s$, and $A_p = A_a = A_s$ because the sensor and actuator have the same size and are of the same material. In equation (2.6), $r_a = (h_a + h)/2$ is the effective moment arm, $d_{31,a}$ is a piezoelectric constant of the actuator, $r_s = (h_s + h)/2$, $h_{31,s}$ is a piezoelectric constant of the sensor, h is the beam thickness, and h_s is the sensor thickness. The output voltage of a piezoelectric sensor is given by Tzou [1]

$$\varphi_s(t) = \frac{h_s}{x_{s2} - x_{s1}} h_{31,s} r_s \left(\frac{\partial w}{\partial x} \right)_{x_{s1}}^{x_{s2}} \quad (2.7) \text{ In}$$

order to achieve more effective vibration control, the sensor signal is amplified by a gain G and the resulting signal sent to the actuator is

$$\varphi_a(t) = G\varphi_s(t) \quad (2.8)$$

The cantilever beam is clamped at $x=0$ resulting in zero displacement and slope. The beam is free at $x=l$ giving zero shear and zero resultant moment. This results in the following boundary conditions for $t > 0$

$$w(0,t) = 0, \quad \frac{\partial w}{\partial x} \Big|_{x=0} = 0 \quad (2.9)$$

$$\left[\alpha(x) \frac{\partial^2 w}{\partial x^2} \right]_{x=l} = 0, \quad \left[\frac{\partial}{\partial x} \left(\alpha(x) \frac{\partial^2 w}{\partial x^2} \right) \right]_{x=l} = 0 \quad (2.10)$$

3. FREE VIBRATION ANALYSIS

Standard free vibration analysis is performed on the beam. The transverse motion of the beam is a function of both position and time and is given by

$$w(x,t) = \psi(x)e^{\lambda t} \quad (3.1)$$

where $\lambda = i\omega$. Taking the partial derivatives of $w(x,t)$ and substituting them into the equation of motion gives

$$\lambda^2 \rho(x)\psi(x) + L[\psi(x)] = 0 \quad (3.2)$$

4. INTEGRAL EQUATION SOLUTION

An analytic solution to equation (3.2) for a beam with collocated piezo sensor and actuator patches is proposed. An integral equation is introduced and it will be shown that the eigensolutions of the integral equation are eigensolutions to the equation of motion. Consider the following integral equation

$$\sigma\psi(x) = \int_0^l \rho(s)K(x,s)\psi(s)ds \quad (4.1)$$

where $\sigma = \omega^2$ and the kernel is given by

$$K(x,s) = G(x,s) + p(x)q(s) \quad (4.2)$$

where $G(x,s)$, $p(x)$, and $q(s)$ are auxiliary functions. The auxiliary functions are chosen such that they satisfy the following conditions

$$L[K(x,s)] = \delta(x-s) \quad (4.3a)$$

$$\frac{\partial^2}{\partial x^2} \left(\alpha(x) \frac{\partial^2 G(x,s)}{\partial x^2} \right) = \delta(x-s) \quad (4.3b)$$

$$\frac{d^2}{dx^2} \left(\alpha(x) \frac{d^2 p(x)}{dx^2} \right) = S''(x) \quad (4.3c)$$

4.1 Equivalence

Using the relationship (4.3a), it can be shown that the eigensolutions to the integral equation are eigensolutions of the differential equation of motion given by equation (3.2). This is demonstrated in the following manner:

Assume $\psi(x)$ to be a solution of the integral equation (4.1) and apply the L operator to both sides of the integral equation (4.1), then one obtains

$$\sigma L[\psi(x)] = \int_0^l L[K(x,s)]\rho(s)\psi(s)ds \quad (4.4)$$

Using the condition (4.3a) and the fundamental property of the delta function, the equation (4.4) can be reduced to

$$\sigma L[\psi(x)] = \rho(x)\psi(x) \quad (4.5)$$

which takes the same form as the differential equation given by (3.2). Hence with an appropriately chosen kernel and auxiliary functions $G(x,s)$, $p(x)$, and $q(s)$, the eigensolutions of the integral equation are eigensolutions of the equation of motion.

4.2 The $q(s)$ Function

To determine $q(s)$, the relationships defined in equations (2.2), (4.2) and (4.3b-c), are used to write $L[K(x,s)]$ as

$$L[K(x,s)] = \frac{\partial^2}{\partial x^2} \left[\alpha(x) \left(\frac{\partial^2 G}{\partial x^2} + q(s) \frac{\partial^2 p}{\partial x^2} \right) - b\xi \left[\frac{\partial^2 G}{\partial x^2} \Big|_{x_{s1}} + q(s) \frac{\partial^2 p}{\partial x^2} \Big|_{x_{s1}} \right] \right] S^*(x) \quad (4.6)$$

Solving equations (4.3a)- (4.6) for $q(s)$ yields the following

$$q(s) = \frac{b\xi [G_x(x_{s2},s) - G_x(x_{s1},s)]}{1 - b\xi [p_x(x_{s2}) - p_x(x_{s1})]} \quad (4.7)$$

4.3 The $p(x)$ Function

To determine the patch function $p(x)$, the following relationship is used

$$\frac{d^2}{dx^2} \left(\alpha(x) \frac{d^2 p}{dx^2} \right) = H''(x - x_{a1}) - H''(x - x_{a2}) \quad (4.8)$$

Upon integrating equation (4.8) twice results in

$$\alpha(x) \frac{d^2 p}{dx^2} = H(x - x_{a1}) - H(x - x_{a2}) \quad (4.9)$$

with the constants of integration being equal to zero. The solution of equation (4.9) is a piecewise function comprised of the following

$$p(x) = \begin{cases} 0 & 0 \leq x < x_{a1} \\ p_1(x) & x_{a1} \leq x \leq x_{a2} \\ p_2(x) & x_{a2} < x \leq l \end{cases} \quad (4.10)$$

where $p_1(x)$ is a quadratic function and $p_2(x)$ is a linear function. The functions $p_1(x)$ and $p_2(x)$ are given by

$$p_1(x) = \frac{(1/2)(x - x_{a1})^2}{E_b I_b + 2E_p I_p} \quad (4.11a)$$

$$p_2(x) = \frac{[(x_{a2} - x_{a1})(x - x_{a2}) + (1/2)(x_{a2} - x_{a1})^2]}{E_b I_b + 2E_p I_p} \quad (4.12b)$$

which are only valid for aligned sensor and actuator patches ($x_{s1} = x_{a1}$ and $x_{s2} = x_{a2}$).

4.4 The $G(x,s)$ Function

The last auxiliary functions to be determined are the $G(x,s)$ and $g(x,s)$ functions. Let $g(x,s)$ be defined as

$$g(x,s) = \hat{g}(x,s)H(s-x) + g(s,x)H(x-s) \quad (4.13)$$

The function $\hat{g}(x,s)$ is chosen such that $g_{xxxx}(x,s) = \delta(x-s)$. For a cantilever beam, a function for $\hat{g}(x,s)$ which satisfies this condition is

$$\hat{g}(x,s) = -\frac{1}{6}x^3 + \frac{1}{2}sx^2 \quad x < s \quad (4.14a)$$

$$\hat{g}(s,x) = -\frac{1}{6}s^3 + \frac{1}{2}xs^2 \quad x > s \quad (4.14b)$$

Using the following relationship, $G(x,s)$ can be determined

$$\frac{\partial^2}{\partial x^2} \left[\alpha(x) \frac{\partial^2 G(x,s)}{\partial x^2} \right] = g_{xxxx}(x,s) \quad (4.15)$$

Integrating equation (4.15) twice results in the following

$$G_{xx}(x,s) = g_{\eta\eta}(\eta,s)\alpha^{-1}(\eta) \quad (4.16a)$$

$$G_x(x,s) = \int_0^x g_{\eta\eta}(\eta,s)\alpha^{-1}(\eta)d\eta \quad (4.16b)$$

$$G(x,s) = \int_0^x (x-\eta)\alpha^{-1}(\eta)g_{\eta\eta}(\eta,s)d\eta \quad (4.16c)$$

where the integration constants are equal to zero.

5. METHOD OF SOLUTION

- a. Choose a complete orthonormal set of functions.
- b. Expand the kernel in terms of the Fourier series of the orthonormal functions.
- c. Reduce the integral equation to an infinite set of linear equations.
- d. Determine the number of terms N such that successive solutions differ by a negligible amount.
- e. Consider the integral equation in which the kernel is replaced by the N -term Fourier series expansion of the kernel.
- f. The new integral equation is reduced to solving a linear system of $N+1$ equations with $N+1$ unknowns.

For the solution of the integral equation, a set of orthonormal eigenfunctions $\phi_n(x)$ is chosen which are those for an uncontrolled beam with no control moment term. The mode shapes of a standard cantilever beam with boundary conditions for a fixed end at $x = 0$ and a free end at $x = l$ are

$$W_n(x) = -\frac{U(\Omega_n)}{T(\Omega_n)}V(\Omega_n x/l) + T(\Omega_n x/l) \quad (5.1)$$

where the eigenvalues are defined by

$$\Omega^4 = (\rho A/EI)l^4 \omega^2 \quad (5.2)$$

in which

$$T(x) = \frac{1}{2}[\sinh(x) - \sin(x)] \quad (5.3a)$$

$$U(x) = \frac{1}{2}[\cosh(x) + \cos(x)] \quad (5.3b)$$

$$V(x) = \frac{1}{2}[\cosh(x) - \cos(x)] \quad (5.3c)$$

The orthonormal eigenfunctions are given by

$$\phi_n(x) = \frac{W_n(x)}{\|W_n(x)\|_{L^2}} \quad (5.4)$$

The function $G(x,s)$ can be expanded in terms of the eigenfunctions $\phi_n(x)$ of the uncontrolled beam

$$G(x,s) = \sum_{j=1}^{\infty} \sum_{k=1}^{\infty} G_{jk} \phi_j(x) \phi_k(s) \quad (5.5)$$

where

$$G_{jk} = \int_0^l \int_0^l G(x,s) \phi_k(x) \phi_j(s) dx ds \quad (5.6)$$

Equation (4.1) in terms of the auxiliary functions and equations (4.2) and (5.6) gives

$$\sigma \psi(x) = \sum_{j=1}^{\infty} \sum_{k=1}^{\infty} G_{jk} \phi_j(x) C_k + p(x) C_{\infty} \quad (5.7)$$

where

$$C_k = \int_0^l \phi_k(s) \psi(s) \rho(s) ds, \quad C_{\infty} = \int_0^l q(s) \psi(s) \rho(s) ds \quad (5.8)$$

To convert equation (5.7) into a set of linear equations capable of being solved, multiply by $\rho(x) \phi_n(x)$ and integrate from 0 to l . Also, equation (5.7) can be multiplied by $\rho(x) q(x)$ and integrated from 0 to l resulting in

$$\sigma C_n = \int_0^l \rho(x) \sum_{j=1}^{\infty} \sum_{k=1}^{\infty} G_{jk} \phi_j(x) \phi_n(x) C_k dx + \int_0^l \rho(x) p(x) \phi_n(x) C_{\infty} dx \quad (5.9)$$

$$\sigma C_{\infty} = \int_0^l \rho(x) \sum_{j=1}^{\infty} \sum_{k=1}^{\infty} G_{jk} \phi_j(x) C_k q(x) dx + \int_0^l \rho(x) p(x) q(x) C_{\infty} dx \quad (5.10)$$

for $n=1,2,\dots,\infty$.

The set of equations can now be solved to determine the eigenvalues (natural frequencies). However, there are an infinite number of terms for the system of equations. A finite number of terms must be selected resulting in a finite set of linear equations. Now the integral equation has been reduced to solving a linear system of $N+1$ equations with $N+1$ unknowns. Once the eigenvalues are obtained, the mode shapes can be found using equation (5.7).

6. FINITE ELEMENT SOLUTION

The finite element method is used as an alternative to the analytic solution obtained from the integral equation approach. A finite element model of a controlled beam is constructed and the corresponding mass and stiffness matrices of the controlled structure are derived. Standard beam elements are used as a foundation for the model and are modified to include the mass and stiffness of the piezo patches and also account for the control moment induced by the piezo actuator patch.

The natural frequencies and normal modes of the controlled beam are obtained by solving the matrix equation

$$[M]\{\ddot{U}\} + [K]\{U\} = \{0\} \quad (6.1)$$

A harmonic solution is assumed for $\{U\}$ in the form

$$\{U\} = \{\bar{U}\} e^{i\omega t} \quad (6.2)$$

resulting in

$$[[K] - \omega^2 [M]]\{\bar{U}\} = \{0\} \quad (6.3)$$

For there to be a nontrivial solution, the determinant of the coefficient matrix of $\{\bar{U}\}$ must be zero

$$[[K] - \omega^2 [M]] = 0 \quad (6.4)$$

The polynomial of equation (6.4) can now be solved to determine the natural frequencies of the system and the mode shapes can then be determined from equation (6.3).

6.1 Finite Element Model

The finite element model uses a combination of beam elements and patch elements. Patch elements are modified beam elements, which are necessary to account for the added stiffness and mass of the piezo patches along with the control effect created by the piezo actuator. Standard beam elements are used for the section of the beam where there are no piezo patches. The approximating function for $w(x,t)$ is given by

$$\tilde{w}(x) = w_1 N_1(x) + \theta_1 N_2(x) + w_2 N_3(x) + \theta_2 N_4(x) \quad (6.5)$$

where w_1 and w_2 are the nodal transverse displacements and θ_1 and θ_2 are the nodal rotations. The shape functions are the standard beam element shape functions

$$N_1(x) = 1 - \frac{3x^2}{l_e^2} + \frac{2x^3}{l_e^3}, \quad N_3(x) = \frac{3x^2}{l_e^2} + \frac{2x^3}{l_e^3} \quad (6.6a)$$

$$N_2(x) = x - \frac{2x^2}{l_e} + \frac{x^3}{l_e^2}, \quad N_4(x) = \frac{x^3}{l_e^2} + \frac{x^2}{l_e} \quad (6.6b)$$

where l_e is the element length.

6.2 Mass Matrices

The consistent mass matrix for a uniform two-node beam element is given by

$$[m]^{(e)} = \int_0^{l_e} \rho A [N]^T [N] dx \quad (6.7)$$

where $[N] = [N_1(x) \ N_2(x) \ N_3(x) \ N_4(x)]$ and is a row matrix containing the shape functions.

(i) Beam Element Mass Matrix with no Piezo Patches

The integral in equation (6.7) can be carried out using $\rho_b A_b$ for the beam density and area and the following matrix is obtained

$$[m_b]^{(e)} = \frac{\rho_b A_b l_e}{420} \begin{bmatrix} 156 & 22l_e & 54 & -13l_e \\ 22l_e & 4l_e^2 & 13l_e & -3l_e^2 \\ 54 & 13l_e & 156 & -22l_e \\ -13l_e & -3l_e^2 & -22l_e & 4l_e^2 \end{bmatrix} \quad (6.8)$$

(ii) Patch Element Mass Matrix with Piezo Patches

This is similar to the mass matrix obtained in equation (6.8) but the masses of the sensor and actuator patches are added to the mass of the beam resulting in

$$[m_p]^{(e)} = \frac{(\rho_b A_b + 2\rho_p A_p) l_e}{420} \begin{bmatrix} 156 & 22l_e & 54 & -13l_e \\ 22l_e & 4l_e^2 & 13l_e & -3l_e^2 \\ 54 & 13l_e & 156 & -22l_e \\ -13l_e & -3l_e^2 & -22l_e & 4l_e^2 \end{bmatrix} \quad (6.9)$$

6.3 Stiffness Matrices

The stiffness matrix for a beam element is obtained using the integral

$$[k]^{(e)} = \int_0^{l_e} [B]^T EI [B] dx \quad (6.10)$$

where $[B]$ is the second derivative of $[N]$ with respect to x .

(i) Beam Element Stiffness Matrix with no Piezo Patches

The integral in equation (6.10) can be evaluated using $E_b I_b$ as the stiffness of the beam to determine the stiffness matrix for a beam element with no piezo patches

$$[k]_{bending}^{(e)} = \frac{E_b I_b}{l_e^3} \begin{bmatrix} 12 & 6l_e & -12 & 6l_e \\ 6l_e & 4l_e^2 & -6l_e & 2l_e^2 \\ -12 & -6l_e & 12 & -6l_e \\ 6l_e & 2l_e^2 & -6l_e & 4l_e^2 \end{bmatrix} \quad (6.11)$$

(ii) Patch Element Stiffness Matrix with Piezo patches

$$[k_p]^{(e)} = [k]_{bending}^{(e)} + [k]_{control}^{(e)} \quad (6.12)$$

where $[k]_{bending}^{(e)}$ is given by (6.11) and $[k]_{control}^{(e)}$ will be derived in the following section.

6.4 Control Matrix

To determine the control component of the stiffness matrix, the control term is multiplied by the shape functions and integrated

$$\int_0^{l_e} -b\xi \left(\frac{\partial w}{\partial x} \right)_{x_{s1}}^{x_{s2}} [H''(x-x_{a1}) - H''(x-x_{a2})] \bar{N}_i(x) dx \quad (6.13)$$

for $i=1,2,\dots,N_n$ where N_n is the number of nodes and $\bar{N}_i(x)$ are the interpolating functions defined over the entire domain. Substituting the derivatives of the shape functions into the approximating function and evaluating at x_{s1} and x_{s2} which in terms of local element coordinates is $\eta = 0$ and $\eta = l_e$ where $\eta = (x - x_{s1})$

$$\frac{d\tilde{w}}{dx} \Big|_0^{l_e} = [w_1 N_1'(l_e) + \theta_1 N_2'(l_e) + w_2 N_3'(l_e) + \theta_2 N_4'(l_e)] - [w_1 N_1'(0) + \theta_1 N_2'(0) + w_2 N_3'(0) + \theta_2 N_4'(0)] \quad (6.14)$$

For a one element patch

$$N_1'(0) = N_3'(0) = N_4'(0) = 0, N_1'(l_e) = N_2'(l_e) = N_3'(l_e) = 0, N_2'(0) = 1, N_4'(l_e) = 1 \quad (6.15)$$

Substitute equations (6.14)-(6.15) back into the original integral given in equation (6.13) and integrate the result by parts to obtain

$$b\xi (\theta_2 - \theta_1) \left[\int_0^{l_e} \bar{N}_i'(x) S'(x) dx - \bar{N}_i(x) S'(x) \Big|_0^{l_e} \right] \quad (6.16)$$

Using equations (6.16) and the fact that $S'(0)=S'(l)=0$, $S'(x)=[\delta(x-x_{a1})-\delta(x-x_{a2})]$, and $\eta=0$ and $\eta=l_e$ with $\eta=(x-x_{a1})$, the control component of the stiffness matrix becomes the following for a single element piezo patch

$$[k]_{control}^{(e)} = \begin{bmatrix} 0 & 0 & 0 & 0 \\ 0 & -b\xi & 0 & b\xi \\ 0 & 0 & 0 & 0 \\ 0 & b\xi & 0 & -b\xi \end{bmatrix} \quad (6.17)$$

The patch element stiffness matrix with stiffness (6.11) and control components (6.17) is then determined by equation (6.12).

7. NUMERICAL RESULTS

To validate the integral equation solution, the results obtained from the integral equation solution will be compared with the finite element results. An example with collocated piezoceramic (PZT) sensor and actuator patches will be studied. The first three natural frequencies, first three mode shapes, and tip displacement given initial displacement and velocity will be shown.

Computer simulations using the Maple 9.5 software package are performed to obtain the results. The set of equations from equations (5.9) and (5.10) must be truncated to a finite set of equations in order to achieve a numerical solution. It is found that a six term solution ($N=5$) produces accurate results. A finite element code is also written in Maple 9.5 to find the natural frequencies of the controlled structure. A ten element model is used where the beam is divided up into 0.1l element lengths. It was found that when ten elements are used, the frequencies were converging and not changing much when more elements are added. The mode shapes for the first two case studies are also found using a Maple 9.5 program.

The structure consists of an aluminum beam with PZT-5H sensor and actuator patches. The material properties and dimensions of the beam and piezo patches are similar to the experiment performed by Xu and Koko [7] and are listed in Table I. For the analysis performed, only collocated sensor and actuator positions are considered. The sensor and actuator also have the same physical properties, i.e. $E_p=E_a=E_s$, $\rho_p=\rho_a=\rho_s$, and $h_p=h_a=h_s$.

Table I: Properties of beam and piezo patches

Beam Properties		
Elastic Modulus	E_b	68 GPa
Density	ρ_b	2800 kg/m ³
Width	b	0.025 m
Height	h_b	0.965 mm
Length	l	0.226 m
PZT Properties		
Elastic Modulus	E_p	61 GPa
Density	ρ_p	7500 kg/m ³
Width	b	0.025 m
Height	h_p	0.75 mm
Piezo Constants	d_{31}	274x10 ⁻¹² V/m
	h_{31}	5.5x10 ⁸ V/m

CASE I. The Piezo Patches at Collocated Locations $x_{s1}=x_{a1}=0.1l$ and $x_{s2}=x_{a2}=0.3l$.

The frequencies found from the integral equation and the finite element solutions for this case are presented in Table II. The first three natural frequencies for various gain values are shown.

Table II: Natural frequency results

Gain		Integral Equation (rad/sec)	Finite Element (rad/sec)
0	ω_1	120.13	120.11
	ω_2	515.57	516.75
	ω_3	1455.44	1469.50
50	ω_1	122.27	122.26
	ω_2	515.62	516.80
	ω_3	1480.31	1494.96
250	ω_1	122.77	122.76
	ω_2	515.64	516.82
	ω_3	1486.18	1500.95
500	ω_1	122.85	122.84
	ω_2	515.64	516.82
	ω_3	1487.11	1501.91

The first three mode shapes for this case using displacement feedback control determined from the integral equation solution and the finite element solution are displayed in Fig. 2. The finite element mode is represented by dashed line while a solid line represents the mode shape obtained from the integral equation.

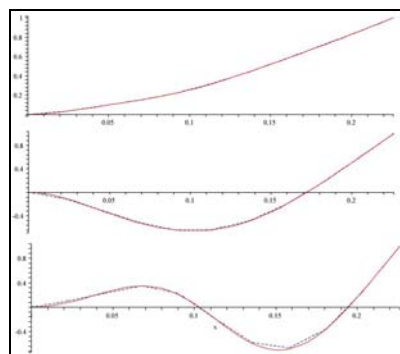


Fig. 2 First Three Mode shapes

CASE II: Various Patch Configurations

The first three natural frequencies using the integral equation solution for collocated patches starting near the base of the beam with $x_{a1}=x_{s1}=10^{-6}l$ and extending in 0.1l increments are listed in Table III.

Table III: Natural frequencies for various patch locations (rad/sec)

Gain		$x_{a2} = x_{s2}$ Patch Locations			
		0.2l	0.3l	0.4l	0.5l
0	ω_1	141.27	176.15	220.25	265.71
	ω_2	852.93	939.60	838.16	721.46
	ω_3	2225.05	3559.43	1849.16	2258.34
50	ω_1	146.08	188.42	249.99	337.63
	ω_2	904.31	1111.54	1099.97	842.23
	ω_3	2482.14	2205.17	1852.44	2355.77
100	ω_1	147.23	191.51	258.09	360.90
	ω_2	917.36	1163.39	1247.12	919.34
	ω_3	2544.33	2432.96	1855.53	2421.69
500	ω_1	147.42	192.01	259.42	364.84
	ω_2	919.47	1171.87	1278.02	936.05
	ω_3	2553.89	2483.27	1856.38	2436.40

8. CONCLUSION

Analytic and finite element solutions are obtained for two case studies using displacement feedback control. The first three natural frequencies and mode shapes are found for the integral equation and finite element solutions. No analytic solution existed previously for a controlled beam that includes the mass and stiffness of the piezo patches or no experiment has been performed to find the natural frequency of a controlled structure with piezoceramic patches. Since there was no experimental data to compare the analytic solution to, a finite element model is used to verify the integral equation solution. The natural frequency results for the two case studies obtained from the integral equation solution matched very closely with the finite element solution, therefore verifying the analytic solution. The mode shapes found for Cases I and II using the integral equation solution also matched very closely with the finite element solution.

REFERENCES

- [1] S. Tzou, "Piezoelectric Shells," Kluwer Academic Publishers, 1993.
- [2] H. T. Banks, D.J. Inman, D. J. Leo, and Y. Wang, "An experimentally validated detection theory in smart structures," *Journal of Sound and Vibration*, vol. 191, 1996, pp. 859-880.
- [3] N. D. Maxwell, and S. F. Asokanathan, "Modal characteristics of a flexible beam with multiple distributed actuators," *Journal of Sound and Vibration*, vol. 269, 2004, pp. 19-31.
- [4] J. Tani, S. Chonan, Y. Liu, F. Takahashi, K. Ohtomo, and Y. Fuda, Y., "Digital active vibration control of a cantilever beam with piezoelectric actuators," *JSME International Journal*, vol. 34, 1991, pp.168-175.
- [5] J. M. Sloss, J.C. Bruch, Jr., S. Adali, and I. S. Sadek, "Piezoelectric patch control using an integral equation approach," *Thin-Walled Structures*, vol. 39, 2001, pp. 45-63.
- [6] J. M. Sloss, J.C. Bruch, Jr., S. Adali, and I. S. Sadek, "Integral equation approach for beams with multi-patch piezo sensors and actuators," *Journal of Vibration and Control*, vol. 8, 2002, pp. 503-526.
- [7] S. X. Xu, and T.S. Koko, "Finite element analysis and design of actively controlled piezoelectric smart structures," *Finite Elements in Analysis and Design*, vol. 40, 2004, pp. 241-262